Available online freely at www.isisn.org

Bioscience Research

Print ISSN: 1811-9506 Online ISSN: 2218-3973

Journal by Innovative Scientific Information & Services Network

RESEARCH ARTICLE BIOSCIENCE RESEARCH, 2021 18(SI-2)131-144 **OPEN ACCESS**

Physicochemical properties of rose cactus (Pereskia bleo) mucilage and pea protein isolate complex coacervates as a function of mixing ratio.

Nor Alia Che Nozid [1], Nor Hayati Ibrahim [1*], Sakinah Harith [2]

[1]Faculty of Fisheries and Food Science, Universiti Malaysia Terengganu, 21030 Kuala Nerus, Terengganu, **Malaysia**
[2]Faculty of Health Science, Universiti Sultan Zainal Abidin, Kampung Gong Badak, 21300 Terengganu, **Malaysia**

***Correspondence:** yati@umt.edu.my **Received 05-07-00-2021, Revised: 12-08-2021, Accepted: 15-08-2021 e-Published: 19-08-2021**

Rose cactus mucilage (RCM) obtained from the leaves of *Pereskia bleo,* is one of the potential hydrocolloids having a characteristic of anionic polysaccharide that could form a complex coacervate with the oppositely-charged proteins including pea protein isolate (PPI). Thus, coacervates have drawn attention for their ability to effectively encapsulate bioactive ingredients within the emulsion-based delivery system. However, this RCM-PPI interaction might be influenced by their mixing ratio which in turn would affect the overall coacervate functionalities in the emulsion. This study aimed to determine the physicochemical properties (zeta potential, turbidity, coacervate yield, emulsifying properties, and droplet microstructure) of complex coacervates based on RCM and PPI at different mixing ratios (RCM: PPI; 0:10 to 10:0). It was confirmed that RCM has a characteristic of anionic polysaccharide with zeta potential values of -7.8 to -11.7 mV measured at pH 3 to 4. Based on this fact, the 2% RCM-PPI complex coacervates were then prepared at pH 3.60 (±0.09) for optimum coacervation. There were no significant effects ($p > 0.05$) of mixing ratios on zeta potential, yield, and turbidity, but there were significant effects ($p < 0.05$) on emulsifying properties of the RCM-PPI coacervates. The mixing ratio at 8:2 was found to significantly ($p < 0.05$) increase the emulsion stability of the RCM-PPI coacervate. At this mixing ratio, the RCM-PPI coacervates also exhibited zeta potential, yield, turbidity, emulsifying capacity, and also emulsion stability of -9.5 mV, 25.68%, 1.40, 27.11%, and 24.71% respectively. The optimum coacervation was further characterized by agglomeration and dense structure of coacervates observed under the light microscope. FTIR spectrum of the coacervates revealed a contribution of hydrogen bonds at 3316 cm^{-1}, corresponding to significant interaction between RCM and PPI at the mixing ratio of 8:2. This study suggested higher fraction of protein in mixing ratios are preferable for optimum coacervation, ensuring better functionality in the emulsion system.

Keywords: Rose cactus mucilage, pea protein isolate, mixing ratio, coacervate, interaction

INTRODUCTION

Rose cactus (*Pereskia bleo*) is a tropical herb under Cactaceae family but with leafy cactus (Wahab et al. 2009) which is believed to have the ability for treatment of certain diseases such as cancer-related disease (Hong et al. 2012). *Pereskia bleo* consists of 3.03% of mucilaginous materials (Aluwi et al. 2019) known as Rose cactus mucilage (RCM). This mucilage is proven to have a very high water holding capacity (461.87%) which contributes to its gelling properties (Hong et al. 2012) that may help in stabilization of emulsion. However, protein found in RCM was in the form of arabinogalactan-protein (AGP) (Aluwi et al. 2019) which only comprises 10% of amino acid and over 90% of carbohydrate

(Waldron and Faulds, 2007). Thus, in relation to medicinal purposes, to prepare unique emulsion-based food products stabilized solely by RCM and at the same time, there is needs for dietary protein to be supplemented, additional protein from other source seems to be of crucial.

In the food and beverage industry, pea protein has earned great attention due to its high nutritional content (Wei et al. 2020). Plant protein such as pea protein isolate (PPI) is derived from split yellow field peas. Peas (*Pisum sativum* L.) are second major crucial leguminous crop which can be discovered over 25 million acres globally. It is prevalent in many countries such as Canada, China, United States, Russia, and France in their diet as it is known for having 18-30% protein with greater amount of tryptophan and lysine compared to cereal grains (Lan et al. 2018; Shevkani et al. 2015). Major proteins constituent found in PPI were albumins and two globulins which functionalised on surface properties in hydrocolloid system such as oil binding capacity, hydrophobicity, and emulsification (Boye et al. 2010; Freitas et al. 2000; Lan et al. 2018). Despite their benefits, protein-stabilized emulsions are extremely vulnerable to environmental stresses such as pH, ionic strength, and temperature, impacting encapsulated compounds (Burgos-Díaz et al. 2016). PPI also has high hydrophobic surface structure, smaller surface charge, and low water-solubility resulted in protein instability (e.g. aggregation and precipitation) in aqueous solution or dispersion, which is a major impediment in emulsion systems (Karaca et al. 2011).

Hence, this study approaches the interactions between polysaccharides and proteins that affect positively on the rheological properties (Freitas et al. 2017) as well as the physical stability of the emulsion compared to a single biopolymer (Xiong et al. 2018). The blend of polysaccharides and proteins results in the formation of electrostatically attracted moieties known as complex coacervates (Hasanvand and Rafe, 2018). Complex coacervation is known as associative interaction between different charge molecules carried by functional groups of proteins and polysaccharides, resulting in the formation of a polymeric phase in equilibrium with another aqueous phase upon separation (Gupta et al. 2012). Theoretically, coacervation between protein-polysaccharide form between the polysaccharide pKa and protein isoelectric point (pI) (Liu et al. 2017). Coacervate can improve emulsion stabilizing ability of the protein, thus it has been utilised to be used in food that are not capable on achieving emulsion stability just by using the polysaccharide and protein alone (Xiong et al. 2018). It also can coat like a thin film of dispersed droplets, thus prevents coalescence (Caballero et al. 2003) of emulsion system.

The majority of emulsions in industrial manufacturing are stabilised by mixing emulsifiers with plant polysaccharides (Shao et al. 2020). However, this combination (complex coacervate) depends on few factors such as the entire mixed hydrocolloid concentration, pressure (shear force) temperature, and the mixing ratios between biopolymer mixture (Gupta et al. 2012). According to Klemmer et al. (2012), the combination between PPI and alginate polysaccharides showed maximum coacervation at low pH and high protein fraction in the mixing ratio that affects their physicochemical characteristics. These good fundamental insights into PPI-polysaccharide coacervation reflect the possibility of RCM and PPI coacervation yet it has not been studied so far. Therefore, this study focused on determination of physicochemical properties of binary biopolymer systems of RCM and PPI as affected by different mixing ratios (0:10 to 10:0; RCM: PPI), aiming for an optimum coacervation.

MATERIALS AND METHODS

Materials

Mature green fresh leaves of rose cactus mucilage (RCM) were picked from a controlled site in Universiti Malaysia Terengganu (Longitude 5°24’53.3” N, Latitude 103°04’59.1” E), Kuala Terengganu. Pea protein isolate (PPI) was purchased from Sigma Aldrich Company. All chemicals utilised in this study were of analytical grade.

Extraction and purification of mucilage

Rose cactus leaves were soaked for 3 hours in a 0.14M sodium hydroxide solution at a 1:3 w/w ratio and homogenised at lower speed for 45 seconds. The extraction solution was heated in water bath for 45 minutes at 70°C and cooled to room temperature before proceeding to centrifuge at 8000 rpm for 15 minutes at 25°C. Next, the crude mucilage was precipitated from the supernatant with ratio 1:3 (w/w) of acetone then dried overnight in an oven at 40°C (Oven Memmert, Germany). The dried crude mucilage was obtained and undergo pulverisation by using a waring blender. For purification, crude RCM was dispersed and stirred (250 rpm) in deionised water (1% w/v) for 30 minutes at 70°C. The dispersion

was precipitated using saturated barium hydroxide at ratio 1:3 (w/w) and stirred for 5 minutes at 25 °C with speed 250 rpm. The sample-solvent slurry was allowed to stand for 30 minutes before undergo centrifuged at 10,000 rpm for 15 minutes. Filtration was conducted to obtain the precipitate, which was then washed twice with saturated barium hydroxide and acetone. The purification process was completed after it was dried in an oven overnight (40°C). The dried purified mucilage was collected and pulverised by using a waring blender. The yield of purified mucilage was determined by using the formula below (Aluwi et al. 2019):

$$\text{Yield percentage}(\%) = \frac{\text{Weight of dried purified mucilage (g)}}{\text{Weight of dried crude mucilage used (g)}} \times 100$$

Determination of moisture content, crude protein, and ash content of mucilage.

Crude protein of RCM was discovered using the Kjeldahl method (conversion factor of 6.25) and ash content was obtained using standard AOAC 1990 (AOAC, 1990). Moisture content was collected by drying empty crucible in an oven (Oven Memmert, Germany) overnight at 105 °C and rested in a desiccator to ensure complete moisture removal. The crucible was weighted, then 2 g of sample was placed into the crucible and dried for 24 hours at 105 °C until fully dry. Before being weighed, the sample was cooled in a desiccator. The yield was weighed and the percentage of moisture content was calculated by using the formula below (modified from Amin et al. 2007):

$$\text{Dry sample percentage}(\%) = \frac{\text{Weight of dried sample (g)}}{\text{Weight of sample (2g)}} \times 100$$

$$\text{Moisture content percentage}(\%) = 100\ \% - \text{dried sample percentage}(\%)$$

Stock solution preparation

Stocks solution of individual RCM and PPI were prepared at (2% w/v) by stirring with a magnetic stirrer at speed 450 rpm for 5 minutes at ambient temperature (25+1°C). The stock solutions were heated up to 80°C for RCM, whereas PPI was kept at 25°C for 2 hours at continuous stirring speed 450 rpm on a thermostated hot-plate. The stock solutions were left overnight to ensure complete hydration (Aluwi et al. 2015).

Determination of zeta potential of individual biopolymer

Zeta potential was measured by electrophoretic light scattering (ELS) by using Litesizer 500 (Anton Paar, Austria) which measures the speed of the particles within the presence of an electrical field. RCM and PPI were prepared at 0.2% (v/v) from stock solution of 2% (v/v). The measurements were taken at different pH range 2 to 9 (±0.09) by adjusting using HCL 1 N and NaOH 1 N. The individual sample was loaded into a specific cuvette called Omega Cuvette and reading was measured at 25 °C and voltage of 200 V (modified from Albano et al. 2018).

Biopolymer mixture preparation

Stock solutions of RCM and PPI were prepared as stated before. Biopolymer mixture at different mixing ratios (RCM: PPI); (0:10, 1:9, 2:8, 3:7, 6:4, 7:3, 8:2, 9:1, 10:0) were investigated in correlation with coacervation yield at fixed pH 3.6 (±0.09) by adjusting using HCL 1 N and NaOH 1 N before undergo ultrasonic homogeniser. The biopolymer mixtures were introduced to ultrasonic homogeniser at amplitude 20, 30 and 40 for 2 minutes each. pH was adjusted to pH 3.6 again before complete homogenisation. Biopolymer mixtures were then diluted with deionised water at ratio 1:10 to a concentration of 0.2% (v/v) for zeta potential, and turbidity measurement. No dilution was applied for droplet microstructure, emulsifying properties, and complex coacervate yield test.

Determination of zeta potential (charge density)

Zeta potentials of biopolymer mixtures were similarly measured by electrophoretic light scattering as described before.

Determination of turbidity

The soluble complexes can be determined via turbidimetric techniques. The turbidity on the equilibrium phase was collected using a UV-Vis spectrophotometer (UV-1700 Pharmaspec Shimadzu, Kyoto, Japan) at a wavelength of 600 nm at 25(±1°C). Samples were positioned in 1 cm path length cuvettes and absorbance values were recorded after 1 minute (Espinosa-Andrews et al. 2007).

Determination of coacervate yield

2% (w/v) of biopolymer mixtures were mixed by using an ultrasonic homogeniser. No dilution was applied as the amount of acid required to

adjust electrical equivalence pH value did not vary significantly ($p > 0.1$) on dry coacervate yield (Daniels et al. 1995). After the complex coacervation process, samples were centrifuged to force phase-separated at 10,000 rpm for 15 minutes and the coacervates-free top phase (supernatant) was carefully removed, and the bottom phase with precipitated coacervates was oven-dried for 12-18 hours at 103 ± 2 ˚C. The coacervation yields were collected based on formula below (modified from Daniels et al. 1995; Ghadermazi et al. 2019):

$$\text{Percentage of coacervation yield,} = \frac{\text{Coacervate dry mass recovered (g)}}{\text{Total mass of biopolymer used (g)}} \times 100$$

Determination of emulsifying properties

The biopolymer mixtures (2% w/v) were combined with commercial corn oil with ratio 1:2 (w/w). Mixed aqueous solutions were homogenised using an ultrasonic homogeniser at amplitude 20, 30 and 40 for 2 minutes each. The emulsifying capacity was obtained by using the following calculation (Aluwi et al. 2019; Sciarini et al. 2009):

$$\text{Emulsifying capacity percentage (\%),} = \frac{\text{Height of emulsion layer (cm)}}{\text{Height of whole sample (cm)}} \times 100$$

The emulsion stability was acquired by heating the emulsion in a water bath (Techne 12/ TE – 10D) at 80 °C for 30 minutes. Then, the suspensions were centrifuged (800 rpm) for duration of 10 minutes. The emulsion stability was determined by using the following formula (Aluwi et al. 2019; Sciarini et al. 2009):

$$\text{Emulsion stability percentage (\%),} = \frac{\text{Height of emulsion layer (cm)}}{\text{Height of whole sample (cm)}} \times 100$$

Determination of droplet microstructure

The biopolymer mixtures were placed over a glass slide as small drops with a cover slip and observed at low magnification of 40× using a phase contrast microscope using Microscope Eye Piece Camera (Olympus BH-2 microscope, Tokyo, Japan) together with CX2 Olympus Microscope. The images of the sample were recorded via a manual camera and pictures were stored on a computer. The microstructure images were analysed using Olympus BH-2 microscope, Tokyo, Japan (Logaraj, 2010).

Determination of functional groups by Fourier Transform Infrared Spectroscopy (FTIR)

The procedure was adapted from Raei et al. (2018) with a slight modification. The biopolymer mixtures samples were positioned on ray exposing stage of Fourier Transform Infrared Spectrophotometer (IRTracer-100 Shimadzu, Kyoto, Japan) which operated at 4 cm^{-1} spectral resolution. Spectrum of each sample was recorded in the wavelength range of 400–4000 cm^{-1} on average of 16 scans in ATR mode (attenuated total reflectance). Analyses were conducted at ambient temperature (25 °C) and the background was collected prior every sample was measured. By taking the negative of the log ratio of a sample spectrum to that of air, the spectra were transformed to absorbance units.

Statistical analysis

All experiments were carried out at least duplicate and reported on mean ± standard deviation. Significant effects of independent variables on the physicochemical properties and functional properties were analysed by implementing a One-Way ANOVA with Tukey's Multiple Comparison using a Minitab 18 (Minitab Inc., USA) statistical software at $\alpha = 0.05$.

RESULTS AND DISCUSSION

Chemical properties of mucilage

Based on Table 1, purified RCM using saturated barium hydroxide showed high protein content (20.91%). This result was comparable to previous research conducted by Aluwi et al. (2019) on purified RCM using saturated barium hydroxide which resulted in 26.01% of protein content. This finding could be supported by Martin et al. (2017) who researched on protein content of purified *Pereskia aculeata* which exhibited 19.00% protein content. In contrast, crude RCM contained only 9.11% protein content (Aluwi et al. 2019). The increase in protein content of RCM might be due to the method of extraction and purification that used high pH medium (alkaline conditions) and moderate temperature. If a low pH medium was used for extraction and purification, protein content might decrease due to molecular hydrolysis induced by the acid (Karazhiyan et al. 2011). Moreover, the temperature used for extraction and purification was not too high which only 70 °C, as it could prevent further protein denaturation that might lead to reduction of protein content due to loosening of covalent bond in arabinogalactan-protein (Ibrahim et al. 2019).

High protein content in RCM was remarkable for the present study as high protein was acknowledged to contribute to emulsifying properties (Hong et al. 2012). Protein is assumed to be bound to carbohydrates as glycoproteins (Ibrahim et al. 2019) known as arabinogalactan-protein (Aluwi et al. 2019). Physical purification on crude mucilage is impossible to eliminate this arabinogalactan-protein as it is stable against alkaline mediums (Aluwi et al. 2019). Theoretically, fat, fiber and ash content of mucilage will be reduced after purification but not the protein content due to its bond with monosaccharide units of mucilage and the bond is also believed to stronger after purification (Aluwi et al. 2019)

Ash content shows the existence of inorganic matter in the materials which involve mineral content and heavy metals (Bhushette et al. 2017). Table 1 displays high ash content of RCM. Comparable results were observed for *Opuntia ficus-indica* mucilage (20.08%) (Gebresamuel et al. 2011), *Opuntia ficus-indica* mucilage (33.96%) (Espino‐Díaz et al. 2010), and *Opuntia stricta* mucilage (29.93%) (Gebresamuel et al. 2011). So, it could be concluded that, plant from Cactaceae family contains high inorganic materials. The different value of chemical compositions in RCM mucilage could be attributed by the species diversity and diverse growth environments of plants (Razmkhah et al. 2016). However, as referred to the previous study done by Aluwi et al. (2019) on a similar purification medium of RCM, their result showed a substantial decrease in ash content from crude to purified RCM (28.11% to 10.11%).

Table 1 shows that the moisture content of RCM was low (8.99%). In contrast, a study was done by Hong et al. (2012) on moisture of crude RCM showed relatively high moisture content which was 13.69% compared to this study on purified RCM. This might be due to double exposure to drying during the extraction and purification process for purified RCM. However, the moisture content of RCM in the present study was quite similar to a previous study conducted by Hosseini-Parvar et al. (2010) on *Ocimum basilicum L.* seed gum which resulted in 9.1% of moisture content. Low moisture contents were also observed on *Lepidium perfoliatum* seed gum (6.0%) (Koocheki et al. 2013), Linseed mucilage, Basil mucilage, Dragon head mucilage, and Quince mucilage (4.38 – 4.93%) (Fekri et al. 2008). On the other hand, higher moisture contents were observed on mucilage of *Opuntia ficus-indica* mucilage and *Opuntia stricta* mucilage i.e. 11.57-12.43% and 11.72% respectively (Espino‐Díaz et al. 2010; Gebresamuel et al. 2011).

Table 1: Moisture content, protein content, and ash content of RCM.

Chemical Properties	Rose cactus mucilage
Moisture Content (%)	8.99 ± 0.11
Protein Content (%)	20.91 ± 0.70
Ash Content (%)	24.96 ± 1.67

Values are mean ± standard deviation from three replications (n=3).

Zeta potential of individual polysaccharide and protein

Figure 1 presents the effect of pH on zeta potential values of RCM and PPI solutions. This study, for the first time demonstrated that RCM is an anionic polysaccharide, as it exhibited negative charge of zeta potential value (-7.8 mV to -21.7 mV) from pH 3.06 to pH 9.07. Based on a study conducted by Aluwi et al. (2019), four crucial monosaccharides found in crude and purified RCM were galactose, mannose (1070-810 cm^{-1}), arabinose (1068- 830 cm-1), and galacturonic acid (uronic acid) (1740-1210 cm^{-1}) in different amounts. They also revealed that RCM was a polysaccharide as it contained β-(1→4)-D-glucosidic main backbone which was negatively charged but not at very low pH where the carboxyl groups dissociation was suppressed. Based on these facts, the anionic behaviour of RCM was believed to be contributed by galacturonic acid (uronic acid) having a carboxyl (-COOH) group as part of their structure (Martin et al. 2017). This result was coincided with Freitas et al. (2017), who indicated that increase in pH value of polysaccharides solutions resulted in increased negative charge corresponding to anionic behaviour until this value reached a plateau.

However, protein-based emulsifier, PPI showed a different behaviour as it reached the isoelectric point (pI). The pI is the pH in which zeta potential is zero and the particles carry no net charge. Below its pI, proteins appeared to have positive charges whereas beyond this point showing negative charges. Figure 1 displays that PPI dispersion went from positive charge (+23.8 mV to +16.9 mV) at pH 2.05 to pH 4.08 and negative charge (-3.0 mV to -18.7 mV) at pH 5.03 to pH 9.00. Lan et al. (2018) observed a similar result as PPI went from positive charge at pH 3 (+32.3 mV) to negative charge at pH 7 (-32.8 mV). These protein particles carried no net charge at

pH 4.0 to pH 5.0 which was similar to the research done by Lan et al. (2018), stating that the pI of PPI was around pH 4.6. In addition, protein structure highly depends on pH which was proven by a study conducted by Ducel et al. (2005), they found a monodispersed random coil behaviour of α-gliadin affected by changing pH. The pH of the solvent is also one of the factors that affect charges of polysaccharide chain, based on pKa value of its reactive site. More polysaccharide dissociation is inhibited at lower pH values; therefore, no additional complexation can be detected. The net repulsion system becomes unstable at high concentrations because biopolymers repel each other, a phenomenon termed as thermodynamic incompatibility. This condition occurs when the pH of the system was higher than protein pI at greater ionic strength (Ghosh et al. 2012). Hence, by altering the pH of medium, one could control polysaccharides-protein interaction.

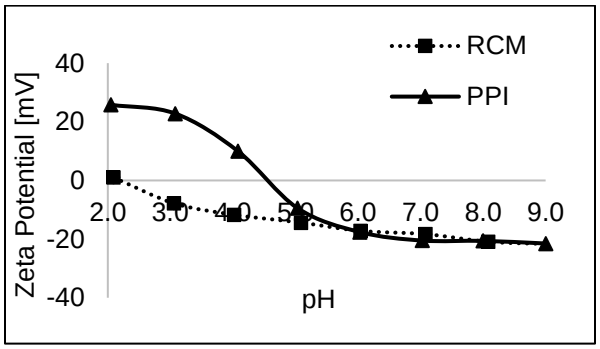

Figure 1: Effect of pH on zeta potential (mV) of 0.2% (w/v) solutions of RCM and PPI.

Based on the zeta potential results, one could select the most suitable pH range where polysaccharide is negatively charged while protein carries positive charges. From this finding, an early conclusion could be made that interaction of RCM and PPI best occurred at pH 3.4 – 3.6 as there was a possibility of complex formation and presentation of attractive interaction on the ground that they had opposite charges and at relatively high values (Freitas et al. 2017). This could be supported by Liu et al. (2009) and as they proved that interaction of PPI and gum Arabic at biopolymer mixing ratio of 1:1 best occurred at pH 3.5. This fact coincides with Lan et al. (2018), who discovered maximum optical density between PPI- high methoxyl pectin (HMP) at ~pH 3.6 where a homogenous one phase was detected, likely owing to the formation of soluble complexes between negatively charged HMP and patches of positive charges on the surface of PPI molecules. Differently, at pH 4.1 and above, RCM and PPI carried the same charges. This pH was not suitable for biopolymer coacervation as both RCM and PPI showed the same anionic behaviour which could cause segregative phase behaviour, whereby the system will split into protein and polysaccharide rich phases.

Zeta potential of biopolymer mixture (charge density)

Complex coacervate formation depends on a few factors such as the entire biopolymer concentration, pressure (shear force), temperature, and the mixing ratios between biopolymer mixture. Moreover, the charge distribution of both biopolymers influences the strength of complexation (Gupta et al. 2012). Figure 2 indicates that net charge of biopolymer mixtures containing RCM and PPI resulted in negative net charge as affected by various mixing ratios. Higher polysaccharide fraction in the mixing ratios indicated that fewer protein molecules were accessible to interact with polysaccharide chains. The interaction is due to electrostatic linking between anionic carboxyl groups of RCM and cationic amino groups on the protein surface contributed to the formation of complexes system (Lan et al. 2018). Figure 2 shows that PPI at ratio 0:10 carried positive charge at pH 3.6 as it was below its pI. According to Souza et al. (2017), zeta potential for mixture of polysaccharide and protein should be intermediate between values of the individual polymer. This behaviour indicates that proteins with a number of reactive sites will bind easily to polysaccharide chains at pH lower than its pI value. However, this finding was not in accord with the previous findings as zeta potential values of RCM-PPI were not intermediate between the values of individual polymers accross all various mixing ratios. Most importantly, a sudden drop of the zeta potential values towards negative charges but close to 0 mV, when the PPI being mixed with RCM fairly justified the biopolymer coacervation reaction did occur.

The zeta potential of RCM-PPI coacervates at mixing ratios of 1:9 to 9:1 were observed to be close to zero but still carried negative net charges. This condition probably occurred due to a positive charge of protein that is not adequate to bind all negative RCM carboxyl groups (Souza et al. 2017). This condition can also be called coacervate phase as there is strong electrostatic

interaction between the polymers resulting in low net charge (Gulão et al. 2014). According to Liu et al. (2009), at pH 3.6 with mixing ratio 1:2 of polysaccharide-protein in the absence of added salt, coacervation of PPI-gum Arabic was found to be at an optimal condition. This was due to interactions between both biopolymer resulting in zero net charge; zeta potential equal to 0 mV.

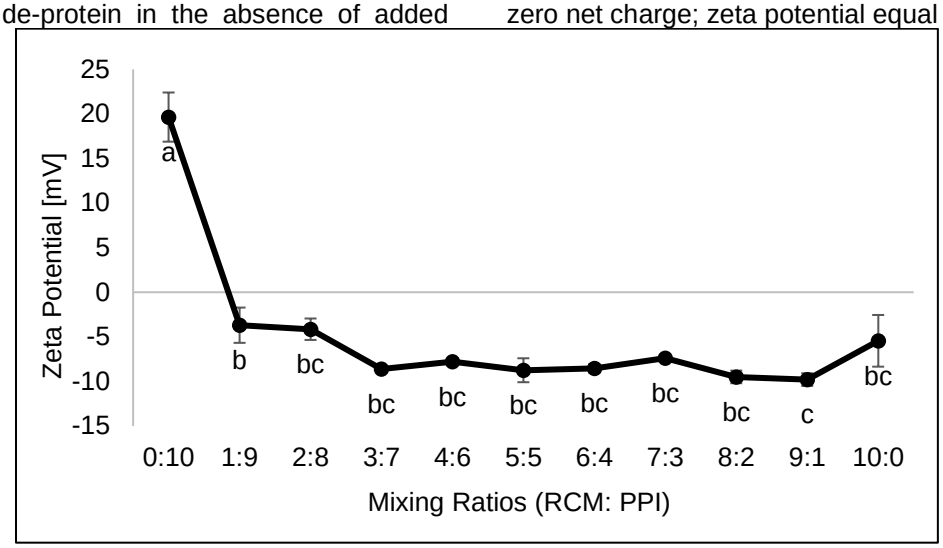

Figure 2: Effect of different mixing ratios of biopolymer mixture (RCM-PPI) on zeta potential. Data represent the means ± standard deviation, n = 2. [a-c] Means with the same letter are not significantly different.

Another study done by Rampazzo et al. (2017) stated that, decreased zeta potential values of Kraft Pulp-Cellulose nanocrystal (KP-CNC) due to increase in viscosity value which influenced the mobility of electrophoretic in the electric field. This finding could support the result displayed in Figure 2 as zeta potential values of biopolymer mixtures were smaller than that individual PPI i.e. mixing ratio of 0:10. This is due to the fact that increases in RCM proportion will increase the overall viscosity of the biopolymer mixtures. However, at mixing ratios of 2:8 to 8:2, the zeta potential values was not significantly different ($p>0.05$) from each other. Significant differences ($p<0.05$) were only noticed between the mixing ratio of 1:9 and 9:1, with the highest PPI and RCM proportions, respectively.

Turbidity and coacervate yield of biopolymer mixture

Turbidity measurement was done in this study to visualize the optimum coacervation existed in the biopolymer mixtures. Figure 3 depicts high PPI portion in RCM-PPI coacervate showed high absorbance values measured at 600 nm. High turbidity indicates cloudy appearance of the mixture which may interpret there is coacervate formation at these mixing ratios resulting in insoluble precipitates (Gulão et al. 2014). The presence of turbidity is due to appearance of scattering molecules or droplets in the mediums, which correlate to coacervate development. If formation of coacervate occured, increases in quantity and size of coacervate will result in turbid solution that scatters the light (Liu et al. 2017).

Ducel et al. (2004) mentioned in their research, light scattering is influenced by few factors such as sizes of dispersed particles, light wavelength, and refractive index of molecules as related by its medium and molecule concentration. Therefore, changes in turbidity values are considered as there are formation or dissociation of polysaccharide and protein coacervates in the mixed bioplymer system (Ru et al. 2012). Study done by Gulão et al. (2014), higher turbidity indicated the formation of stable colloidal suspension of polysaccharides-protein, which encouraged dispersion of light. As stated by Liu et al. (2009), near protein isoelectric point (pI), soluble polysaccharide-protein formed as a slight increase of turbidity was noticed on gum Arabic – pea protein isolate (AG-PPI) complex. However, for the present case, from ratios 1:9 to 9:1, the absorbance values of RCM-PPI coacervates have no significant difference ($p>0.05$) among each other, indicating a similar extent of coacervation regardless the mixing ratio.

The coacervate yield was determined in this research to understand the effect of various

mixing ratios between protein and polysaccharides on efficiency of complex coacervate formation. During the analysis, the coacervates phase remained viscous-like even after phase separation, quite close to the findings by Espinosa-Andrews et al. (2007) who investigated the interaction between Arabic gum and chitosan. The highest coacervate yield from Figure 4 was at ratios 1:9 which scored 29.68% but not significantly different ($p > 0.05$) across all mixing ratios. The highest coacervate yield was due to the strongest electrostatic interaction between positive amino groups (NH_3^+) of protein and negative carboxyl groups of mucilage (Tavares et al. 2020). Higher RCM portion in mixing ratios was observed to contribute higher coacervate yield as compared to mixing ratios with higher PPI portion.

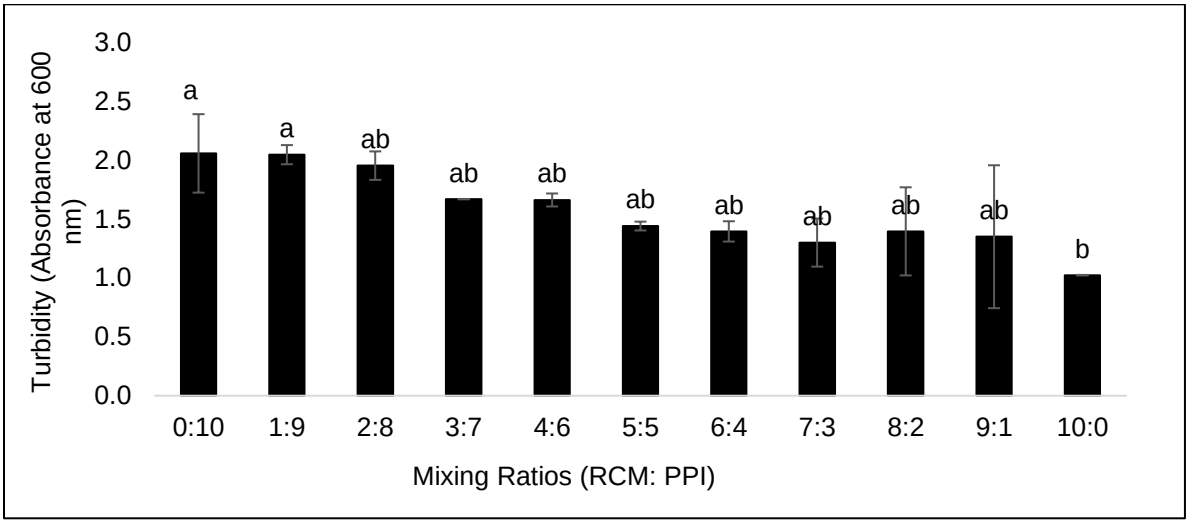

Figure 3: Influence of different mixing ratios of biopolymer mixture (RCM-PPI) on turbidity (absorbance 600 nm). Data represent the means ± standard deviation, n = 2. [a-b] Means with the same letter are not significantly different.

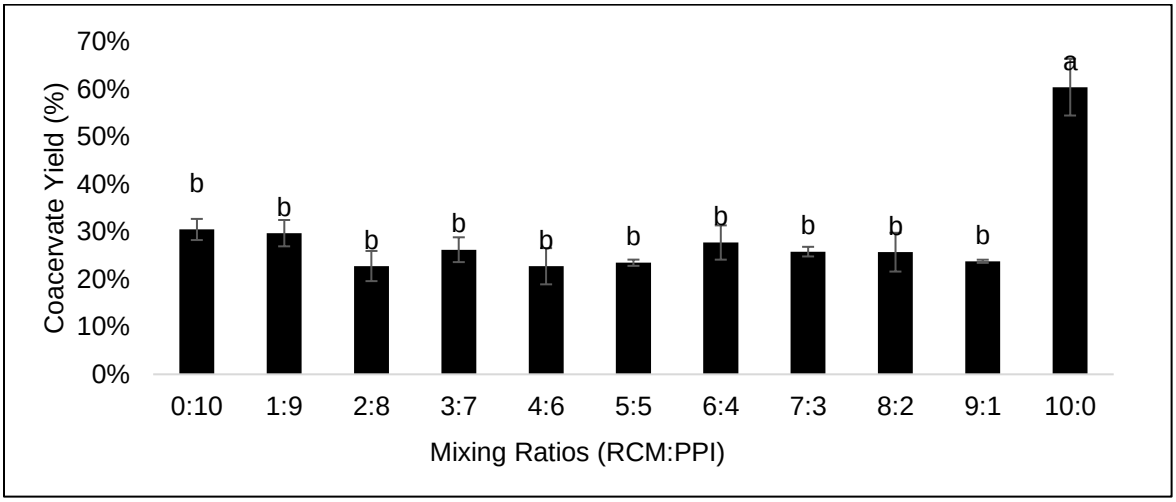

Figure 4: The coacervate yield of biopolymer mixture of RCM-PPI as a function of mixing ratios. Data represent the means ± standard deviation, n = 2. [a-b] Means with the same letter are not significantly different.

It should be mentioned that both turbidity value and coacervate yield are interrelated to each other when considering the contribution of number and size of the cocervate particles. It seemed that both results exhibited a close trend with generally higher PPI proportion in the mixing ratio gave higher values. Unfortunately, since there were no significant differences found across the mixing ratios of 1:9 – 9:1, both measurements could not suggest the best mixing ratio for an optimum RCM-PPI coacervation. Further analysis focusing on the functional properties of the coacervates is thus crucial to be done. This includes emulsifying properties which are discussed in the following section.

Emulsifying properties of biopolymer mixture

Emulsifying capacity is the ability of molecules to serve as agents that ease solubilization or dispersion of two unmixable liquids whereas emulsion stability refer to the capability to maintain an emulsion and its endurance to rupture (Alfredo et al. 2009). Figure 5 shows the emulsifying capacity of RCM-PPI at varied mixing ratios increased significantly ($p<0.05$), resulting in increases from 12.43% to 33.35% as the RCM proportion increased. Likewise, Figure 6 represents the emulsion stability of RCM-PPI that increased significantly from 7.93% to 24.71% with increasing RCM proportion in the mixing ratios. Aluwi et al. (2019) discovered, the emulsifying capability of RCM was most likely dependent on a small fraction of surface-active proteins bound to the strongly branched polysaccharides, most likely in the form of an arabinogalactan-protein complex, as in this case (Hong et al. 2012) which might emulsify the oil into distributed smaller droplets by bridging the hydrophilic barrier at the oil-water interphase. Aluwi et al. (2019) also concluded that, content of uronic acid in the purified RCM would promote better emulsifying properties due to presence of surface activity that generated strong electrostatic repulsion among oil droplets.

In general, the ratio of polysaccharide to protein in a mixture affects their charge balance thus affecting the complex coacervation behaviour (Yuan et al. 2017). Hydrophobic protein chains would adsorb onto the surface of oil droplets due to presentation of non-polar radical amino acids while hydrophilic polysaccharide fractions hinder flocculation and coalescence of oil droplets through steric and/or repulsive electrostatic forces (Aluwi et al. 2019; Ibrahim et al. 2019).

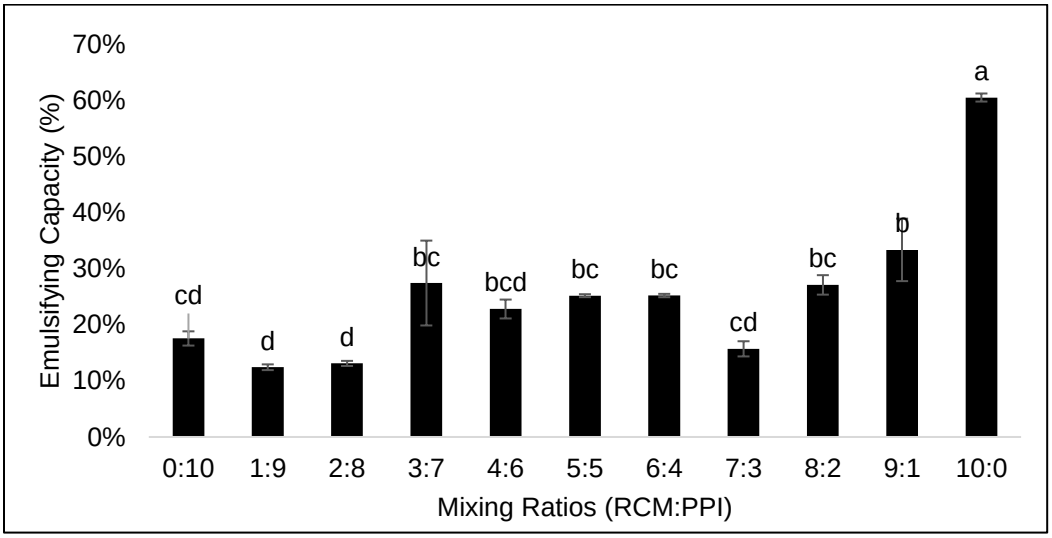

Figure 5: The emulsifying capacity of biopolymer mixture RCM-PPI as a function of mixing ratios. Data represent the means ± standard deviation, n = 2. [a-d] Means with the same letter are not significantly different.

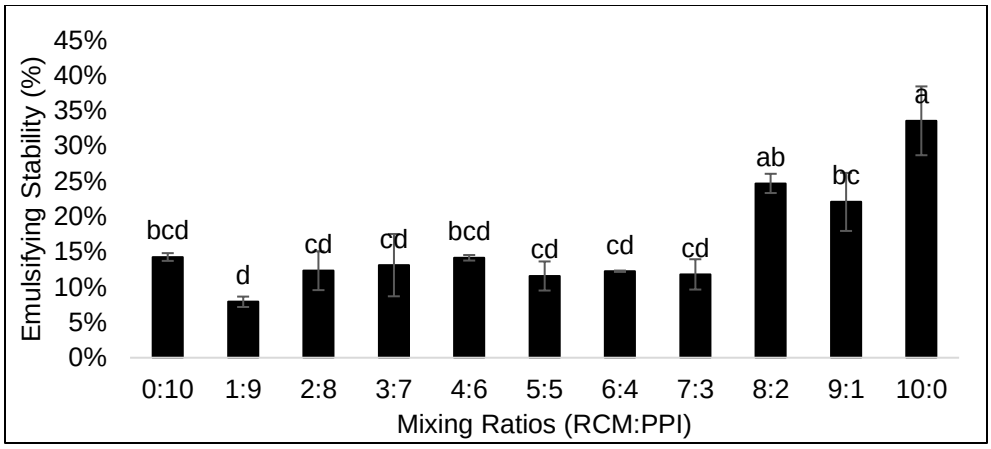

Figure 6: The emulsifying stability of biopolymer mixture of RCM-PPI as a function of mixing ratios. Data represent the means ± standard deviation, n = 2. [a-d] Means with the same letter are not significantly different.

Based on earlier analysis on Figure 2, the biopolymer mixture prepared in this study was in acidic conditions (pH 3.6) which contribute to high electrostatic interaction between the polymers thus promoting their coacervation formation. This explained high emulsion capacity and better stability in mixing ratios with higher RCM portion. Aluwi et al. (2019) reported increasing concentration of RCM from 0.2 to 1%, resulting in better emulsifying capacity and stability from 9.06 – 14.11% and 7.41 – 10.44% respectively. This study revealed quite the same behaviour but with more higher emulsion capacity and stability; 60.51% and 33.59% respectively suggested due to the different pH medium that affect the strength of electrostatic interaction. Most prominently, the emulsion stability results revealed that at the mixing ratio of 8:2, coacervates formed in the system could provide the best functionality as the emulsion stability (24.71%) was significantly ($p < 0.05$) higher than mixing ratio of 1:9 (higher protein proportion) (7.93%).

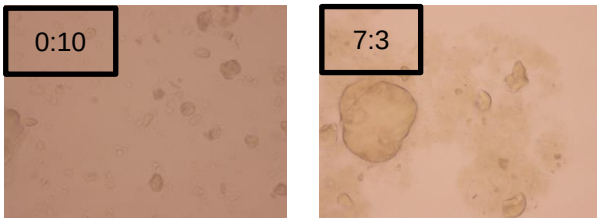

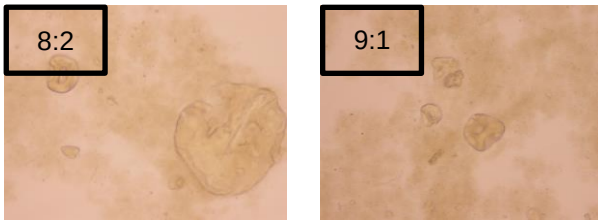

Figure 7: Droplet microstructure of RCM-PPI coacervate (40x magnification) at mixing ratio of 0:10 7:3, 8:2, and 9:1.

Droplet microstructure of biopolymer mixture

Figure 7 shows coacervates agglomerated as large particles and dense at mixing ratio of 8:2 compared to ratio 0:10 which showed only individual and small particles (Ghadermazi et al. 2019).

More obvious round shape structures were found at ratio 8:2 compared to ratio 7:3 and 9:1. They had large round shape structures, making it easier to detect coacervation formation as they became agglomerate and dense. Thus, the higher absorbance value (1.40) in earlier analysis suggested due to the increased in the size of the coacervates (Liu et al. 2017) as shown by Figure 7 at this ratio. Yuan et al. (2014) stated that, as turbidity value increased, larger number and size of complex coacervates could be expected. The similar behaviour was detected by Hasanvand et al. (2018) on flaxseed gum-rice bran protein which showing agglomeration of coacervates at pH for maximum turbidity. These results are consistent with the coacervate yield data that reported higher yield (25.68%) in Figure 4.

Functional groups of biopolymer mixture

FTIR analysis was applied to further characterize the RCM-PPI coacervates formed at the best mixing ratio of 8:2. Figure 8 illustrates the spectra obtained for the biopolymer mixture at the mixing ratio of 8:2 in comparison with individual PPI and RCM. In the spectrum of RCM, a wide peak O-H stretching was observed at band 3325 cm^{-1} and a peak of amide I group at band 1639 cm^{-1} due to C=O stretching vibration from acetylated unit -$CONH_2$. This strong peak corresponding to the high protein content in the RCM as proven in the chemical analysis study which resulted in 20.91% of protein content. The broad band at 2118 cm^{-1} linked with the carbonyl species (Carpentier et al. 2021) of the RCM. Referring to PPI, a strong -OH contraction vibration band was observed at peak 3337 cm^{-1} (Carpentier et al. 2021; Lan et al. 2020). PPI also showed presentation of protein absorption band peaks at 1636 cm^{-1} indicating amide I groups due to C=O stretching vibration of the peptide group (Raei et al. 2018). The peak of amide I was attributed by a greater amount of β-sheet structures in the PPI (Carpentier et al. 2021). In the RCM-PPI coacervates, a wide peak O-H stretching was observed at band 3316 cm^{-1} indicating there was hydrogen bonding interaction between RCM and PPI during coacervation process (Hasanvand and Rafe, 2018).

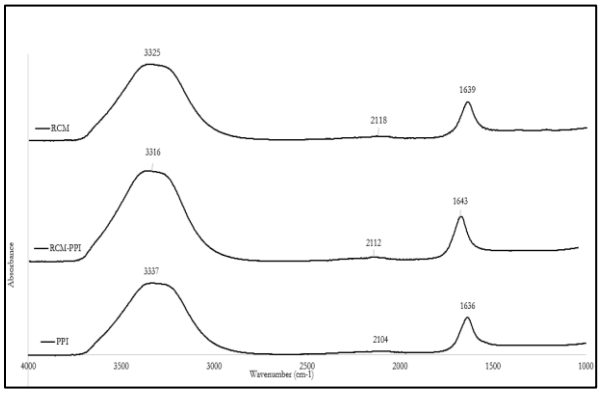

Figure 8: FTIR spectra of RCM, PPI and RCM-PPI at mixing ratio 8:2.

Guerrero et al. (2013) eloquently stated that the hydrogen bonding highly imparted to the development of protein and polysaccharides complex as proven in their studies on interaction between soy protein isolate and agar. Moreover, C-H vibration was discovered at band 2112 cm^{-1} arising from the negatively charged carboxylic groups (Hasanvand and Rafe, 2018) of RCM. RCM-PPI coacervate contributed to band at 1643 cm^{-1} indicating amide I groups due to C=O stretching vibration from acetylated unit -$CONH_2$ (Lan et al. 2020; Lan et al. 2019). These results were in agreement with previous studies on the spectrum of pea protein (Lan et al. 2020; Lan et al. 2019).

CONCLUSION

RCM purified with saturated barium hydroxide has low moisture content, but high in protein and ash content. The protein fraction in RCM was believed to influence its coacervation behaviour upon mixing with PPI. It was discovered that RCM had a characteristic of anionic polysaccharide with zeta potential values of -7.8 to -21.7 mV measured at pH 3 to 9. Moreover, this study revealed that pI of PPI was observed between pH 4.0 to pH 5.0 and the protein carried positive net charge below this value and vice versa. This research showed that the interaction of polysaccharide and protein best occurred at pH 3.4 – 3.6. The particular reason for this pH selection due to RCM and PPI carried different charges at this pH range, thus promoting the complex coacervation. The turbidity and coacervate yield results supported that an appropriate complex coacervation of RCM-PPI had occurred in the mixed biopolymer system. The emulsion stability results suggested that RCM-PPI at the mixing ratio of 8:2 could serve the best functionality of the coacervates in the food colloid system. Moreover, at this mixing ratio, the droplets microstructure revealed particles agglomerated as large particles and dense, indicating an optimum coacervation. This was also well characterized by the FTIR spectrum with the contribution of hydrogen bonds at 3316 cm^{-1} in RCM-PPI (8:2) coacervates indicating their significant electrostatic interaction.

CONFLICT OF INTEREST

None.

ACKNOWLEGEMENT

This study was partly supported by Universiti Malaysia Terengganu.

AUTHOR CONTRIBUTIONS

Nozid NAC: Conducted the study and prepared the manuscript draft.
Ibrahim NH: Designed the study, supervised the study and prepared the manuscript draft.
Harith S: Supervised the study and prepared the manuscript draft.

REFERENCES

Albano, K.M., and Nicoletti, V.R. (2018). Ultrasound impact on whey protein concentrate-pectin complexes and in the O/W emulsions with low oil soybean content stabilization. Ultrasonics Sonochemistry, 41, 562-571.

Alfredo, V.O., Gabriel, R.R., Luis, C.G., and David, B.A. (2009). Physicochemical properties of a fibrous fraction from chia (*Salvia hispanica* L.). LWT-Food Science and Technology, 42(1), 168-173.

Aluwi, N.F.M., Ibrahim, N.H., and Hamzah, Y. (2015). Viscoelastic behavior of polysaccharide blends containing *Pereskia bleo* (Tujuh Duri) mucilage. International Journal of Chemical, Environmental & Biological Sciences, 3(3), 201-205.

Aluwi, N.F.M., Ibrahim, N.H., Hamzah, Y., and Rozaini, M.Z.H. (2019). Chemical and functional properties of rose cactus (*Pereskia bleo*) mucilage as affected by different purification mediums. Asian Journal of Agriculture and Biology, 7(1), 10-18.

Amin, A.M., Ahmad, A.S., Yin, Y.Y., Yahya, N., and Ibrahim, N. (2007). Extraction, purification and characterization of durian (*Durio zibethinus*) seed gum. Food Hydrocolloids, 21(2), 273-279.

AOAC. (1990). Official Methods of Analysis: Fats and Oils.

Bhushette, P.R., and Annapure, U.S. (2017). Comparative study of *Acacia nilotica* exudate gum and acacia gum. International Journal of Biological Macromolecules, 102, 266-271.

Boye, J., Aksay, S., Roufik, S., Ribéreau, S., Mondor, M., Farnworth, E., and Rajamohamed, S. (2010). Comparison of the functional properties of pea, chickpea and lentil protein concentrates processed using ultrafiltration and isoelectric precipitation techniques. Food Research International, 43(2), 537-546.

Burgos-Díaz, C., Wandersleben, T., Marqués, A.M., and Rubilar, M. (2016). Multilayer emulsions stabilized by vegetable proteins and polysaccharides. Current Opinion in Colloid & Interface Science, 25, 51-57.

Caballero, B., Trugo, L.C., and Finglas, P.M. (2003). Encyclopedia of Food Sciences and Nutrition: Academic.

Carpentier, J., Conforto, E., Chaigneau, C., Vendeville, J.-E., and Maugard, T. (2021). Complex coacervation of pea protein isolate and tragacanth gum: Comparative study with commercial polysaccharides. Innovative Food Science & Emerging Technologies, 102641.

Daniels, R., and Mittermaier, E. (1995). Influence of pH adjustment on microcapsules obtained from complex coacervation of gelatin and acacia. Journal of Microencapsulation, 12(6), 591-599.

Ducel, V., Richard, J., Saulnier, P., Popineau, Y., and Boury, F. (2004). Evidence and characterization of complex coacervates containing plant proteins: application to the microencapsulation of oil droplets. Colloids and Surfaces A: Physicochemical and Engineering Aspects, 232(2-3), 239-247.

Ducel, V., Saulnier, P., Richard, J., and Boury, F. (2005). Plant protein–polysaccharide interactions in solutions: application of soft particle analysis and light scattering measurements. Colloids and Surfaces B: Biointerfaces, 41(2-3), 95-102.

Espino-Díaz, M., De Jesús Ornelas-Paz, J., Martínez-Téllez, M.A., Santillán, C., Barbosa-Cánovas, G.V., Zamudio-Flores, P.B., and Olivas, G.I. (2010). Development and characterization of edible films based on mucilage of *Opuntia ficus-Indica* (l.). Journal of Food Science, 75(6), E347-E352.

Espinosa-Andrews, H., Báez-González, J.G., Cruz-Sosa, F., and Vernon-Carter, E.J. (2007). Gum arabic−chitosan complex coacervation. Biomacromolecules, 8(4), 1313-1318.

Fekri, N., Khayami, M., Heidari, R., and Jamee, R. (2008). Chemical analysis of flaxseed, sweet basil, dragon head and quince seed mucilages. Research Journal of Biological Sciences, 3(2), 166-170.

Freitas, L., Ricardo, B.F., Artur, R.T., and Regina. (2000). Use of a single method in the extraction of the seed storage globulins from

several legume species. Application to analyse structural comparisons within the major classes of globulins. International Journal of Food Sciences and Nutrition, 51(5), 341-352.

Freitas, M.L.F., Albano, K.M., and Telis, V.R.N. (2017). Characterization of biopolymers and soy protein isolate-high-methoxyl pectin complex. Polímeros, 27(1), 62-67.

Gebresamuel, N., and Gebre-Mariam, T. (2011). Comparative physico-chemical characterization of the mucilages of two cactus pears (*Opuntia* spp.) obtained from Mekelle, Northern Ethiopia. Journal of Biomaterials and Nanobiotechnology, 3, 79-86.

Ghadermazi, R., Asl, A.K., and Tamjidi, F. (2019). Optimization of whey protein isolate-quince seed mucilage complex coacervation. International Journal of Biological Macromolecules, 131, 368-377.

Ghosh, A.K., and Bandyopadhyay, P. (2012). Polysaccharide-protein interactions and their relevance in food colloids. The Complex World of Polysaccharides, 14, 395-406.

Guerrero, P., Garrido, T., Leceta, I., and de la Caba, K. (2013). Films based on proteins and polysaccharides: Preparation and physical–chemical characterization. European Polymer Journal, 49(11), 3713-3721.

Gulão, E.d.S., de Souza, C.J., da Silva, F.A., Coimbra, J.S., and Garcia-Rojas, E.E. (2014). Complex coacervates obtained from lactoferrin and gum arabic: Formation and characterization. Food Research International, 65, 367-374.

Gupta, R., Basu, S., and Shivhare, U. (2012). A review on thermodynamics and functional properties of complex coacervates. International Journal of Applied Biology and Pharmaceutical Technology, 3, 64-86.

Hasanvand, E., and Rafe, A. (2018). Characterization of flaxseed gum/rice bran protein complex coacervates. Food Biophysics, 13(4), 387-395.

Hasanvand, E., Rafe, A., and Emadzadeh, B. (2018). Phase separation behavior of flaxseed gum and rice bran protein complex coacervates. Food Hydrocolloids, 82, 412-423.

Hong, N.T., and Ibrahim, N.H. (2012). Extraction and characterization of mucilage from leaves of *Pereskia bleo* (Rose cactus)[Ekstraksi dan Karakterisasi Getah Daun Kaktus Mawar (Pereskia bleo)]. Jurnal Teknologi dan Industri Pangan, 23(2), 210.

Hosseini-Parvar, S., Matia-Merino, L., Goh, K., Razavi, S.M.A., and Mortazavi, S.A. (2010). Steady shear flow behavior of gum extracted from *Ocimum basilicum* L. seed: Effect of concentration and temperature. Journal of Food Engineering, 101(3), 236-243.

Ibrahim, N.H., Zakaria, T.N.D.T., and Hamzah, Y. (2019). Optimization of extraction conditions on yield, crude protein content and emulsiying capacity of mucilage from *Talinum paniculatum*. Asian Journal of Agriculture and Biology, 7(1), 156-165.

Karaca, A.C., Low, N., and Nickerson, M. (2011). Emulsifying properties of chickpea, faba bean, lentil and pea proteins produced by isoelectric precipitation and salt extraction. Food Research International, 44(9), 2742-2750.

Karazhiyan, H., Razavi, S.M., and Phillips, G.O. (2011). Extraction optimization of a hydrocolloid extract from cress seed *(Lepidium sativum*) using response surface methodology. Food Hydrocolloids, 25(5), 915-920.

Klemmer, K., Waldner, L., Stone, A., Low, N., and Nickerson, M. (2012). Complex coacervation of pea protein isolate and alginate polysaccharides. Food Chemistry, 130(3), 710-715.

Koocheki, A., Taherian, A.R., and Bostan, A. (2013). Studies on the steady shear flow behavior and functional properties of *Lepidium perfoliatum* seed gum. Food Research International, 50(1), 446-456.

Lan, Y., Chen, B., and Rao, J. (2018). Pea protein isolate–high methoxyl pectin soluble complexes for improving pea protein functionality: Effect of pH, biopolymer ratio and concentrations. Food Hydrocolloids, 80, 245-253.

Lan, Y., Ohm, J.B., Chen, B., and Rao, J. (2020). Phase behavior, thermodynamic and microstructure of concentrated pea protein isolate-pectin mixture: Effect of pH, biopolymer ratio and pectin charge density. Food Hydrocolloids, 101, 105556.

Lan, Y., Xu, M., Ohm, J.B., Chen, B., and Rao, J. (2019). Solid dispersion-based spray-drying improves solubility and mitigates beany flavour of pea protein isolate. Food Chemistry, 278, 665-673.

Liu, J., Shim, Y.Y., Shen, J., Wang, Y., and Reaney, M.J. (2017). Whey protein isolate

and flaxseed (*Linum usitatissimum* L.) gum electrostatic coacervates: Turbidity and rheology. Food Hydrocolloids, 64, 18-27.

Liu, S., Cao, Y.L., Ghosh, S., Rousseau, D., Low, N.H., and Nickerson, M.T. (2009). Intermolecular interactions during complex coacervation of pea protein isolate and gum Arabic. Journal of Agricultural and Food Chemistry, 58(1), 552-556.

Liu, S., Low, N.H., and Nickerson, M.T. (2009). Effect of pH, salt, and biopolymer ratio on the formation of pea protein isolate−gum arabic complexes. Journal of Agricultural and Food Chemistry, 57(4), 1521-1526.

Logaraj, T. (2010). Studies on Selected Plants and Microbes with Special Reference to Polyunsaturated Fatty Acids. University of Mysore.

Martin, A.A., de Freitas, R.A., Sassaki, G.L., Evangelista, P.H.L., and Sierakowski, M.R. (2017). Chemical structure and physical-chemical properties of mucilage from the leaves of *Pereskia aculeata*. Food Hydrocolloids, 70, 20-28.

Raei, M., Rafe, A., and Shahidi, F. (2018). Rheological and structural characteristics of whey protein-pectin complex coacervates. Journal of Food Engineering, 228, 25-31.

Rampazzo, R., Alkan, D., Gazzotti, S., Ortenzi, M.A., Piva, G., and Piergiovanni, L. (2017). Cellulose nanocrystals from lignocellulosic raw materials, for oxygen barrier coatings on food packaging films. Packaging Technology and Science, 30(10), 645-661.

Razmkhah, S., Mohammadifar, M.A., Razavi, S.M.A., and Ale, M.T. (2016). Purification of cress seed (*Lepidium sativum*) gum: Physicochemical characterization and functional properties. Carbohydrate Polymers, 141, 166-174.

Ru, Q., Wang, Y., Lee, J., Ding, Y., and Huang, Q. (2012). Turbidity and rheological properties of bovine serum albumin/pectin coacervates: Effect of salt concentration and initial protein/polysaccharide ratio. Carbohydrate Polymers, 88(3), 838-846.

Sciarini, L., Maldonado, F., Ribotta, P., Perez, G., and Leon, A. (2009). Chemical composition and functional properties of *Gleditsia triacanthos* gum. Food Hydrocolloids, 23(2), 306-313.

Shao, P., Feng, J., Sun, P., Xiang, N., Lu, B., and Qiu, D. (2020). Recent advances in improving stability of food emulsion by plant polysaccharides. Food Research International, 109376.

Shevkani, K., Singh, N., Kaur, A., and Rana, J.C. (2015). Structural and functional characterization of kidney bean and field pea protein isolates: a comparative study. Food Hydrocolloids, 43, 679-689.

Souza, C.J., and Garcia-Rojas, E.E. (2017). Interpolymeric complexing between egg white proteins and xanthan gum: Effect of salt and protein/polysaccharide ratio. Food Hydrocolloids, 66, 268-275.

Tavares, L., and Noreña, C.P.Z. (2020). Encapsulation of ginger essential oil using complex coacervation method: coacervate formation, rheological property, and physicochemical characterization. Food and Bioprocess Technology, 13(8), 1405-1420.

Wahab, S., Abdul, A., Mohan, S., Al-Zubain, A., Elhassan, M., and Ibrahim, M. (2009). Biological activities of *Pereskia bleo* extracts. International Journal of Pharmacology, 5(1), 71-75.

Waldron, K., and Faulds, C. (2007). Cell wall polysaccharides: composition and structure.

Wei, Y., Cai, Z., Wu, M., Guo, Y., Tao, R., Li, R., and Zhang, H. (2020). Comparative studies on the stabilization of pea protein dispersions by using various polysaccharides. Food Hydrocolloids, 98, 105233.

Xiong, W., Ren, C., Tian, M., Yang, X., Li, J., and Li, B. (2018). Emulsion stability and dilatational viscoelasticity of ovalbumin/chitosan complexes at the oil-in-water interface. Food Chemistry, 252, 181-188.

Yuan, Y., Kong, Z.Y., Sun, Y.E., Zeng, Q.Z., and Yang, X.-Q. (2017). Complex coacervation of soy protein with chitosan: Constructing antioxidant microcapsule for algal oil delivery. LWT-Food Science and Technology, 75, 171-179.

Yuan, Y., Wan, Z.L., Yang, X.Q., and Yin, S.W. (2014). Associative interactions between chitosan and soy protein fractions: Effects of pH, mixing ratio, heat treatment and ionic strength. Food Research International, 55, 207-214.